Interactions Mediated by the N-Terminus of Fibrinogen's Bβ Chain †

ARTICLE *in* BIOCHEMISTRY · JANUARY 2007

Impact Factor: 3.02 · DOI: 10.1021/bi061430q · Source: PubMed

4 AUTHORS, INCLUDING:

Rustem I Litvinov
University of Pennsylvania
91 PUBLICATIONS **1,624** CITATIONS

SEE PROFILE

Interactions Mediated by the N-Terminus of Fibrinogen's Bβ Chain†

Oleg V. Gorkun,*,‡ Rustem I. Litvinov,§ Yuri I. Veklich,§ and John W. Weisel§

Department of Pathology and Laboratory Medicine, University of North Carolina School of Medicine, Chapel Hill, North Carolina 27599, and Department of Cell and Developmental Biology, University of Pennsylvania School of Medicine, Philadelphia, Pennsylvania 19104-6058

Received July 14, 2006; Revised Manuscript Received September 29, 2006

ABSTRACT: Specific molecular interactions mediated by the N-terminus of fibrinogen's Bβ chain were revealed using laser tweezers-based force spectroscopy. We examined interactions between fibrinogen fragments representing the center of the molecule, NDSK, desA-NDSK, and desAB-NDSK, and two recombinant fibrinogens, γD364H and γD364A, which have nonfunctional γ-chain polymerization sites to prevent the dominant knob−hole binding. Interactions between desA-NDSK, where the N-terminus of the Bβ chain is present, and the fibrinogen variants showed a complex spectrum of rupture forces which disappeared with desAB-NDSK, lacking both FpA and FpB. The interactions between desA-NDSK and γD364H or γD364A were inhibited by addition of soluble FpB, but not FpA or the polymerization inhibitor peptides GPRP and GHRP. When γD364H fibrinogen was replaced with its X-fragment lacking αC-domains or with fragment D, the strongest component of the rupture force spectrum disappeared, suggesting interactions between the uncleaved FpB and the αC-domain. Electron microscopy confirmed the binding of desA-NDSK to either D or E regions of fibrinogen as well as to αC-domains. The data demonstrate the existence of weak transient interactions within and between fibrin molecules mediated by the N-terminus of the fibrinogen Bβ chain.

Fibrinogen is a key player in hemostasis and wound healing (*1*−*3*). The fibrinogen molecule consists of three pairs of nonidentical polypeptide chains, Aα, Bβ, and γ, linked together by 29 disulfide bonds (*4*). The N-termini of all six chains come together in the central E region of the molecule, while the C-termini of each pair of Aα, Bβ, and γ chains extend outward to form independently folded βC and γC modules at the distal ends of the molecule, called the D regions (Figure 1a). A coiled-coil consisting of all three chains links the globular domains in the middle and ends of the molecule (*5*).

Thrombin converts fibrinogen into fibrin monomer by cleaving short N-terminal sequences of the Aα and Bβ chains called fibrinopeptide A (FpA)[1] and fibrinopeptide B (FpB). The removal of fibrinopeptides exposes the polymerization sites called the 'A' knobs, represented by the GPRV sequence of the α chain, and the 'B' knobs, represented by the GHRP sequence of the β chain (*6*). During clot formation, the newly

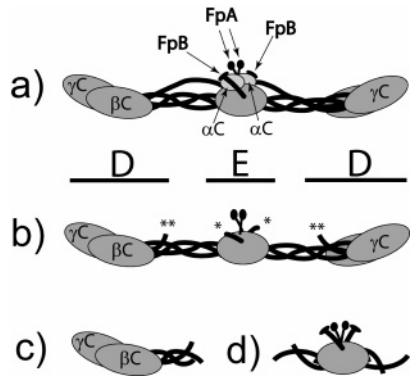

FIGURE 1: Fibrinogen molecule (a) depicted in D−E−D linear arrangement. The two distal D regions consist of γC and βC modules and are connected to the central region E by coiled-coil connectors. The positions of the αC-domains, FpA, and FpB in the center of the molecule are denoted with arrows. Compared to fibrinogen, the X fragment (b) lacks both αC-domains (marked with two asterisks) and parts of the N-terminus of the Bβ chain, including FpB (marked with one asterisk), but preserves the D−E−D arrangement and the N-terminus of the Aα chain, including FpA. The D fragment (c) consists of the βC and γC modules and the coiled-coil connector. The N-terminal disulfide knot (NDSK) represents the E region and consists of the intact N-termini of all six fibrinogen chains (d). Unlike in fibrinogen, X, and D fragments, the coiled-coil connector in NDSK is composed of the Bβ and γ chains only, because the α chain is not long enough to be a part of it.

† This work was supported by National Institutes of Health Grants HL30954 (J.W.W.) and HL 31048 (Susan T. Lord).

* To whom correspondence should be addressed: Department of Pathology and Laboratory Medicine, University of North Carolina School of Medicine, CB#7525 BBB 821, Chapel Hill, NC 27599-7525. Telephone: (919)966-2617. Fax: (919)966-6718. E-mail: ovg@med.unc.edu.

‡ University of North Carolina School of Medicine.

§ University of Pennsylvania School of Medicine.

[1] Abbreviations: NDSK, N-terminal disulfide knot fragment of fibrinogen; desA-NDSK, N-terminal disulfide knot fragment of fibrin with FpA cleaved; desAB-NDSK, N-terminal disulfide knot fragment of fibrin with FpA and FpB cleaved; FpA, fibrinopeptide A; FpB, fibrinopeptide B; γD364H or γD364A, recombinant fibrinogens with Asp substituted with His or Ala, respectively, at position 364 in the γ chain; GPRP, Gly-Pro-Arg-Pro-amide peptide; GHRP, Gly-His-Arg-Pro-amide peptide; CHO, Chinese hamster ovary; SDS−PAGE, sodium dodecyl sulfate−polyacrylamide gel electrophoresis; HEPES, *N*-(2-hydroxyethyl)piperazine-*N*-2-ethanesulfonic acid; HBS, 20 mM HEPES (pH 7.4), 150 mM NaCl buffer; Tris, 2-amino-2-hydroxymethyl-1,3-propanediol; D-γD364H, fragment D of recombinant fibrinogen γD364H; X-γD364H, fragment X of recombinant fibrinogen γD364H; BSA, bovine serum albumin.

10.1021/bi061430q CCC: $33.50
Published on Web 11/16/2006

exposed "knobs" interact with corresponding polymerization "holes" always available in the γC and βC modules (*7*−*10*). This interaction of knobs located in the E region of one molecule with holes located in the D region of another molecule leads to the formation of an intermediate polymer called a protofibril (*1*, *11*, *12*). In the course of polymerization, the protofibrils grow in length and aggregate laterally to form thicker, cablelike fibers (*13*−*15*). The fibers grow in length and diameter and form branches, and at the end, this polymerization process produces the three-dimensional network of a fibrin clot (*16*, *17*).

During thrombin-initiated fibrinogen polymerization, the majority of FpB is cleaved after FpA has been removed (*18*), indicating that the loss of FpA initiates polymerization. This finding, along with other substantive data, supports the model of polymerization in which the A:a "knob−hole" interactions mediate the assembly of protofibrils while the B:b interactions mediate lateral aggregation of protofibrils and formation of fibers (*9*, *19*−*21*). On the other hand, clot formation, including lateral aggregation, occurs in the absence of B:b interactions (*20*, *22*, *23*). Other experiments indicate the N-terminus of the Bβ chain is part of a "composite" polymerization site consisting of sequences from both α and Bβ chains (*24*−*26*). Recently, a peptide representing the Bβ chains [(Bβ1−66)$_2$] was reported to bind to the DD fragment derived from fibrin, suggesting that removal of FpB is not required for interactions between the E and D regions (*27*). Using a laser tweezers instrument, we examined the role of FpB and the N-terminus of the Bβ chain in fibrin polymerization. This instrument measures the discrete rupture forces needed to separate interacting molecules covalently attached to a stationary surface and to a spherical particle trapped in a laser beam (*28*). This experimental design enables the study of individual fibrin−fibrin interactions, circumventing the problem of multiple simultaneous interactions and complications associated with the soluble to insoluble phase change of fibrin polymerization (*29*). We limited the nature of the interacting pairs by using well-defined fibrinogen fragments and variant recombinant fibrinogens (*29*−*32*). Our studies uncovered the existence of weak, transient interactions within and between fibrin(ogen) molecules mediated by the N-terminus of the fibrinogen Bβ chain.

MATERIALS AND METHODS

Materials. All chemicals were reagent grade and purchased from Sigma (St. Louis, MO) unless otherwise specified. FpB, FpA, and GPRP amide (GPRP) peptides were purchased from Bachem USA (Torrance, CA), and GHRP amide (GHRP) was purchased from Biopeptide Co. (San Diego, CA). Latex and silica beads were purchased from Bangs Laboratories, Inc. (Fishers, IN). Cyanogen bromide-activated Sepharose 4B was purchased from Amersham Biosciences (Piscataway, NJ). Monoclonal antibody IF-1 was purchased from KAMIYA Biomedical Co. (Seattle, WA). Human plasma fibrinogen and human α-thrombin were purchased from Enzyme Research Lab (South Bend, IN). Batroxobin (*Batroxobin moojeni*) was purchased from CenterChem (Stamford, CT).

Expression and Purification of Recombinant Fibrinogen. Recombinant fibrinogens γD364H and γD364A were synthesized and purified as previously described (*32*). Briefly, recombinant fibrinogens were expressed in CHO cell lines transfected with cDNA expression vectors encoding normal Aα and Bβ chains and the appropriate mutant γ chain. Cells were grown in serum-free medium in roller bottles. Media containing secreted γD364H or γD364A recombinant fibrinogen were harvested and stored at −80 °C. Fibrinogen was purified from the media by immunoaffinity chromatography with IF-1 antibodies coupled to Sepharose 4B (*31*, *32*). The purified protein was stored in 20 mM HEPES (pH 7.4) and 150 mM NaCl buffer (HBS) at −80 °C. The polypeptide chain composition and the purity of fibrinogen were assessed by sodium dodecyl sulfate−polyacrylamide gel electrophoresis (SDS−PAGE) (Figure 2a). Fibrinogen concentrations were determined by absorption at 280 nm using an extinction coefficient (ε) of 1.5 for a 1 mg/mL solution.

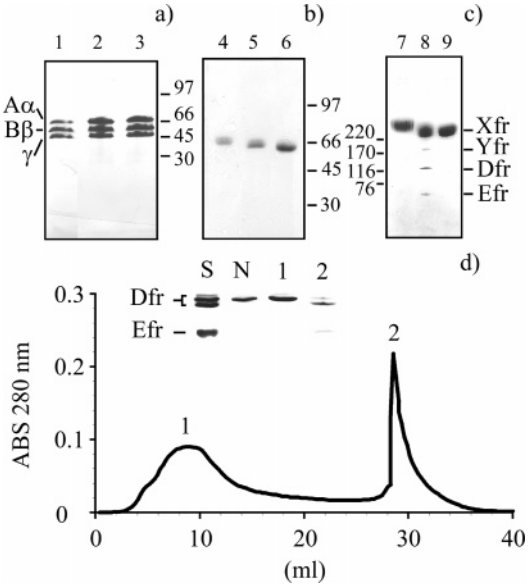

FIGURE 2: SDS−PAGE analysis of (a) reduced samples of fibrinogens in 8 to 25% gradient SDS−PAGE with the position of fibrinogen chains marked at the left, (b) nonreduced samples of NDSK fragments in 12.5% SDS−PAGE, and (c) nonreduced samples of X-γD364H in 4 to 15% gradient SDS−PAGE. The positions of molecular mass markers are indicated on the side of each panel. The order of samples is as follows: wild type recombinant fibrinogen (lane 1), γD364H fibrinogen (lane 2), γD364A fibrinogen (lane 3), NDSK fragment (lane 4), desA-NDSK fragment (lane 5), desAB-NDSK fragment (lane 6), γD364H fibrinogen, nonreduced (lane 7), trypsin digest of γD364H fibrinogen with the order of the fragments indicated at the right (lane 8), and X-γD364H fragment (lane 9). (d) Affinity chromatogram of D-γD364H fragment purification on a GPRPAA affinity column. The inset is an 8 to 25% SDS−PAGE analysis of nonreduced samples of the trypsin digest of γD364H fibrinogen that was loaded onto the column (lane S), the D fragment purified from a trypsin digest of wild type recombinant fibrinogen (lane N), D-γD364H, collected in peak 1 (lane 1), and proteins recovered in peak 2 (lane 2).

Preparation and Purification of Fibrinogen Fragments. The E region of fibrinogen or fibrin can be obtained by cyanogen bromide (CNBr) cleavage (*33*−*35*). This fragment, called the N-terminal disulfide knot or NDSK (Figure 1d), was prepared as described previously (*29*). We prepared three NDSK fragments: NDSK, retaining both FpA and FpB, by CNBr cleavage of human plasma fibrinogen; desA-NDSK, lacking FpA, by CNBr cleavage of fibrin clotted with

batroxobin; and desAB-NDSK, lacking both FpA and FpB, by CNBr cleavage of fibrin clotted with thrombin. All NDSK fragments were purified by size-exclusion chromatography on two sequentially connected Superdex 200 prep grade HR16/50 columns (Amersham-Pharmacia, Piscataway, NJ) equilibrated with 5% acetic acid and 0.1 M NaCl buffer. Purified NDSK fragments were characterized by SDS−PAGE (Figure 2b), dialyzed against HBS, frozen, and stored at −80 °C. NDSK fragment concentrations were determined by absorption at 280 nm using an extinction coefficient (ε) of 0.8 for a 1 mg/mL solution.

Two fibrinogen fragments, X and D (Figure 1b,c), were prepared by trypsin digestion of γD364H fibrinogen, using a modification of the procedure described previously (*8*). Briefly, 20 μL of immobilized TPCK trypsin (Pierce, Rockford, IL) was added to γD364H fibrinogen (2 mg, 0.5 mg/mL) in 20 mM HEPES (pH 7.4), 150 mM NaCl, 20 mM $CaCl_2$ buffer. To prepare fragment X (X-γD364H), the reaction mixture was incubated at room temperature for 1 h and the reaction stopped by filtration through a 0.22 μm filter (Costar, Corning, NY) to separate the trypsin-coated beads from the reaction mixture. The products (4 mL) were loaded onto two sequentially connected Superdex 200 prep grade HR16/50 columns (Amersham-Pharmacia) equilibrated with HBS and eluted at a flow rate of 1 mL/min. Fractions with the X-γD364H fragment, collected between 84 and 94 mL, were identified by molecular mass (∼260 kDa) via SDS−PAGE. Fractions were pooled and the fragments precipitated with an equal volume of saturated ammonium sulfate, and the precipitate was collected at 16 000 rpm for 10 min at 4 °C in an Avanti J25 centrifuge (Beckman-Coulter, Fullerton, CA). The precipitated protein was dissolved in and dialyzed against HBS, characterized by SDS−PAGE (Figure 2c), and stored at −80 °C. The concentration of the X-γD364H fragment was determined by absorption at 280 nm, using an extinction coefficient (ε) of 1.6 for a 1 mg/mL solution.

Fibrinogen fragment D, D-γD364H (Figure 1c), was prepared in the same manner, except it was digested for 2 days at room temperature. The course of the reaction was monitored with the PHAST System (Amersham-Pharmacia) by SDS−PAGE, on 4 to 15% gradient gels. When only bands corresponding to fragments D and E were visible on the gel (Figure 2d inset, lane S), the digestion was stopped by filtration, as described above. The reaction mixture was diluted with an equal volume of water and loaded onto a 2 mL GPRPAA affinity column (*8*) equilibrated with 200 mM Tris (pH 7.4), 20 mM $CaCl_2$ buffer. Under these loading conditions and at a flow rate of 0.2 mL/min, the D-γD364H fragment eluted in the flow-through in a broad peak, while the E fragment bound to the resin (Figure 2d). The peak was collected and the protein concentrated and washed with HBS in a centrifugal filter device (50 kDa molecular mass cutoff; Millipore, Bedford, MA). This concentration−washing step removed low-molecular mass products that contaminated the D-γD364H fragment. The pure fragments, characterized by SDS−PAGE (Figure 2d), were stored at −80 °C. The concentration of the D-γD364H fragment was determined by absorption at 280 nm, using an extinction coefficient (ε) of 2.0 for a 1 mg/mL protein solution.

Electron Microscopy of Fragments and Complexes. Fibrinogen and NDSK fragments were mixed together at a 1:1 molar ratio and a final concentration of 2 μM in 20 mM HEPES buffer (pH 7.4) containing 150 mM NaCl and 3 mM $CaCl_2$. After being incubated at 37 °C for 30 min, samples for electron microscopy were prepared by diluting the protein mixture with a volatile buffer [50 mM ammonium formate (pH 7.4) and 25% glycerol] to a concentration of 20−40 μg/mL and immediately spraying it onto freshly cleaved mica. Sprayed material was rotary shadowed with tungsten in a vacuum evaporator (Denton Vacuum Co., Cherry Hill, NJ) as previously described (*36*, *37*). The presence of glycerol in the sample helps to preserve fibrinogen structure and minimize interaction with the surface (*37*). Prepared specimens were observed in a Philips 400 electron microscope (FEI, Hillsboro, OR) at 80 kV and 60000× magnification. Images were examined from prints of micrographs taken from many different areas of the preparations to obtain a random sample.

Laser Tweezers-Based Model System for Studying Protein−Protein Interactions. The laser tweezers instrument and the model used to study the interaction of individual protein molecules were described in detail previously (*28*, *29*). In brief, interacting proteins were covalently immobilized on two opposite surfaces. One surface (a latex bead) was trapped in a focused laser beam and brought into repeated contact with the other surface (a motionless silica bead covered by a thin layer of polyacrylamide) by moving the laser beam in an oscillatory manner. Upon contact, proteins on the opposite surfaces reacted with each other; however, not every surface contact resulted in specific protein interaction. When interacting proteins were pulled apart, a force arising from the rupture of the established intermolecular bond was measured. The rupture forces (reflecting the strength of protein binding) were collected, normalized by the total number of interaction cycles, and displayed as histograms for each experimental condition.

Coating Surfaces with the Protein. Surfaces coated with the interacting proteins were prepared as described previously (*29*). Each type of NDSK (NDSK, desA-NDSK, and desAB-NDSK) was bound covalently to motionless spherical silica pedestals 5 μm in diameter anchored to the bottom of a chamber. The pedestals were coated with a thin layer of polyacrylamide, then activated with 10% glutaraldehyde (room temperature for 4 h), and washed with 55 mM borate buffer (pH 8.5), and the proteins were allowed to be immobilized overnight at 4 °C from a 1 mg/mL solution in HBS. A solution of 2% BSA in 55 mM borate buffer (pH 8.5) was used as a blocker. In some instances, to form a desAB-NDSK-coated surface, the desA-NDSK was immobilized first and then treated with thrombin (1 unit/mL, 37 °C, 1 h) to cleave FpB, and the reaction chamber was then washed with 20 volumes of 100 mM HEPES (pH 7.4), 150 mM NaCl, 3 mM $CaCl_2$, 2 mg/mL BSA, 0.1% (v/v) Triton X-100 buffer.

Recombinant fibrinogens γD364H and γD364A, fragment X-γD364H, and fragment D-γD364H were bound covalently to carboxylate-modified 1.87 μm latex beads using *N*-[3-(dimethylamino)propyl]-*N*′-ethylcarbodiimide hydrochloride as a cross-linking agent. A solution of 2% BSA in 55 mM borate buffer (pH 8.5) was used as a blocker. The immobilization step lasted 15 min at 4 °C in 55 mM borate buffer (pH 8.5), 150 mM NaCl, and 3 mM $CaCl_2$. The concentration of fibrinogen and fibrinogen fragments in the binding solution was the same (20 μg/mL). When it was

immobilized from a 20 μg/mL solution, the surface density of [^{125}I]fibrinogen was estimated to be approximately (11 ± 2) × 10^{-9} μg/μm^2, which is near the saturation point for surface coverage with bound fibrinogen.

For binding of desA-γD364H fibrin to γD364H fibrinogen, fibrin monomer-coated pedestals were prepared. γD364H fibrinogen (1 mg/mL) was immobilized on spherical silica beads (5 μm in diameter) coated with a thin layer of glutaraldehyde-activated polyacrylamide, repeating the procedure used for the NDSK fragments. Then, the surface-bound γD364H fibrinogen was treated with batroxobin (1 BU/mL, 37 °C, 60 min), and the reaction chamber was then washed with 20 volumes of cold (4 °C) 100 mM HEPES (pH 7.4), 150 mM NaCl, 3 mM $CaCl_2$, 2 mg/mL BSA, 0.1% (v/v) Triton X-100 buffer. The reaction chamber containing desA-γD364H fibrin was prepared fresh, 30 min before each binding experiment.

In a number of experiments, the interacting proteins were immobilized on the opposite surfaces, which did not cause a difference in rupture force profiles. The binding experiments were performed at room temperature in 100 mM HEPES (pH 7.4) containing 150 mM NaCl and 3 mM $CaCl_2$ with 2 mg/mL BSA and 0.1% (v/v) Triton X-100 added to reduce the level of nonspecific interactions.

Measurement of Rupture Forces, Data Processing, and Analysis. The position of the optical trap and hence a protein-coated latex bead was oscillated in a triangular waveform at 0.5 or 1 Hz with a pulling velocity of 1.8 or 3.6 μm/s, which corresponded to a loading rate of 400 or 800 pN/s, respectively. Results obtained at the two loading rates did not differ and, therefore, were combined. All experiments were conducted at a trap stiffness of ~0.22 pN/nm, as computed from the bandwidth of Brownian motion (*28*). The duration of the contact between interacting surfaces varied from 5 to 150 ms. Rupture forces after contact were collected at 2000 scans per second (0.5 ms time resolution). The results of many experiments under similar conditions were averaged so that each rupture force histogram represented from 1 × 10^3 to 3 × 10^4 repeated contacts of more than 10 different bead−pedestal pairs. Individual forces measured during each contact−detachment cycle were collected into 10 pN wide bins. The number of events in each bin was plotted against the average force for that bin after normalizing for the total number of contact−detachment cycles. The percentage of events in a particular force range (bin) represents the probability of rupture events at that force. Optical artifacts observed with or without trapped latex beads produced signals that appeared as forces below 10 pN. Accordingly, rupture forces in this range were not considered when the data were analyzed. Rupture force histograms were empirically fit with a multipeak Gaussian function using Origin 7.5 (Origin Lab Corp., Northampton, MA). The curve fit allowed determination of the position of a peak that corresponds to the most probable rupture force.

RESULTS

Interaction of the N-Terminus of the Bβ Chain from the NDSK Fragment with Fibrinogen. Binding to γD364H fibrinogen was examined for three types of NDSK fragments that differed by their fibrinopeptide composition. Both FpA and FpB were intact in the NDSK fragment; only FpA was missing in desA-NDSK, and both FpA and FpB were missing in desAB-NDSK. For the interaction of the NDSK fragment with γD364H fibrinogen, a multimode rupture force spectrum in the range of 20−120 pN was detected with three peaks at 24 ± 2, 54 ± 1, and 84 ± 3 pN that had a decreasing probability of interaction with stronger forces (Figure 3a). The cumulative probability of all rupture forces of >10 pN was as high as 77 ± 11%. When we replaced NDSK with desA-NDSK, the interaction became more complicated with the advent of additional stronger forces peaking at 111 ± 7 pN (Figure 3b). The cumulative probability of rupture forces of >10 pN for the interaction of desA-NDSK with γD364H fibrinogen was 72 ± 8%. The removal of FpB in addition to FpA caused almost complete abrogation of the interactions of the desAB-NDSK fragment with γD364H fibrinogen (Figure 3c). The range of rupture forces was significantly diminished to 20−60 pN, and the cumulative probability for these interactions dropped to 8 ± 3%. Comparing the histograms depicted in panels a−c of Figure 3, it is clear that the presence of uncleaved FpB was critical for interaction of the NDSK fragments with γD364H fibrinogen.

To verify the effect of removal of FpB on the interaction of the NDSK fragment with γD364H fibrinogen, we treated the surface-bound desA-NDSK with thrombin, which resulted in FpB cleavage and formation of desAB-NDSK directly on the surface. The newly formed desAB-NDSK was then allowed to interact with γD364H. The rupture force spectrum of the interaction of the thrombin-treated desA-NDSK and the γD364H fibrinogen (Figure 3d) appeared as a broad range of forces and was substantially different from the force spectrum of the desA-NDSK fragment (Figure 3b). Although the cumulative probability of the rupture forces of >10 pN was reduced insignificantly (72 ± 12%), the overall force distribution shifted toward lower values and was more typical of that for nonspecific protein−protein interactions, because it did not contain well-defined characteristic peaks (*28*, *38*). It is noteworthy that incomplete inhibition of γD364H binding to thrombin-treated surface-bound desA-NDSK could be a result of incomplete conversion of desA-NDSK into desAB-NDSK since the rate of FpB cleavage from NDSK is much slower than that from fibrinogen, particularly when a protein was immobilized on a surface (*19*, *39*). It is also possible that covalent attachments to the surface preclude surface-bound thrombin-treated desA-NDSK from assuming the same conformation as desAB-NDSK that was formed in solution.

One way to confirm the specificity of the binding reaction between the NDSK fragments and γD364H fibrinogen was to look at the competitive inhibitory effect of free FpB added to the interaction medium. Introduction of 0.1 mM FpB into the binding reaction mixture of desA-NDSK and γD364H fibrinogen resulted in a substantial reduction in the level of binding (Figure 3e). The cumulative probability of the rupture forces of >10 pN was reduced to 46 ± 5% with the force spectrum lacking peaks, typical for specific interaction between fibrinogen and its fragments. The inhibitory effect of FpB introduced into the binding reaction mixture was much more pronounced than that caused by thrombin-induced cleavage of FpB from the surface-bound desA-NDSK (Figure 3d). However, it was not as strong as in the case of the complete absence of FpB in the NDSK molecule

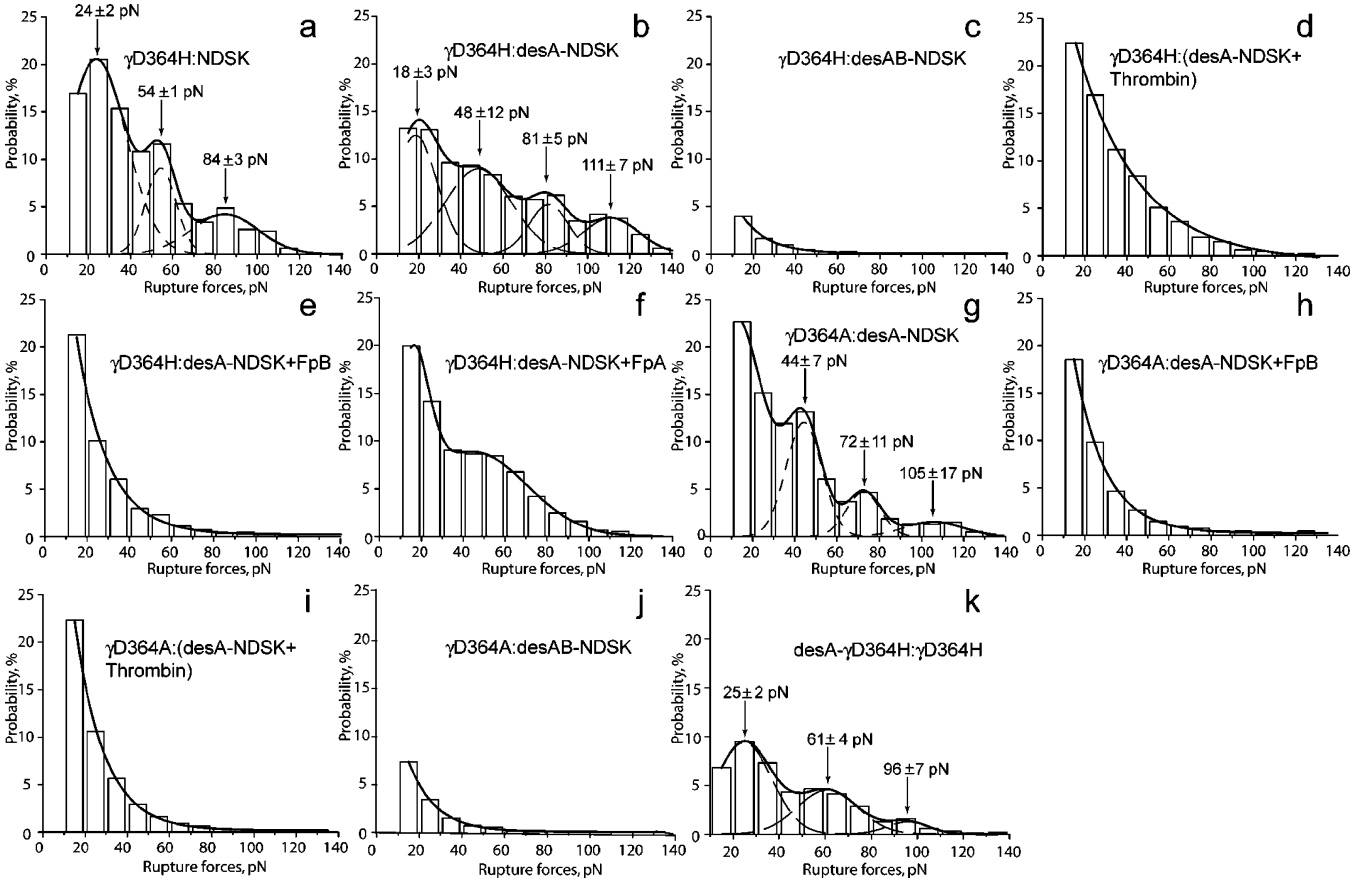

FIGURE 3: Rupture force histograms demonstrating the interactions of different NDSK fragments with fibrinogen variants containing a nonfunctional polymerization hole in the γ chain. The rupture forces were arranged into histograms with 10 pN wide bins and normalized by the total number of counts (*n*) for each experimental condition: (a−c) interactions between fibrinogen γD364H and NDSK ($n = 2135$), desA-NDSK ($n = 6743$), and desAB-NDSK ($n = 5042$), respectively; (d) interactions between fibrinogen γD364H and thrombin-treated desA-NDSK ($n = 1995$); (e and f) interactions between fibrinogen γD364H and desA-NDSK in the presence of 0.1 mM FpB ($n = 2040$) and FpA ($n = 1132$), respectively; (g) interactions between fibrinogen γD364A and desA-NDSK ($n = 3182$); (h) interactions between fibrinogen γD364A and desA-NDSK in the presence of 0.1 mM FpB ($n = 4315$); (i) interactions between fibrinogen γD364A and thrombin-treated desA-NDSK ($n = 2375$); (j) interactions between fibrinogen γD364A and desAB-NDSK ($n = 1371$); and (k) interactions between the surfaces coated with fibrinogen and desA-fibrin γD364H ($n = 1014$).

(Figure 3c). Introduction of free FpA into the binding reaction mixture of desA-NDSK and γD364H fibrinogen also seemed to affect the interaction, but the effect was relatively mild, with a much smaller reduction in the level of binding, compared to that for FpB addition (Figure 3f).

To understand whether the NDSK binding mediated by the N-terminus of the Bβ chain was limited to the specific properties of γD364H fibrinogen, we repeated the binding experiment with γD364A fibrinogen, another variant with an impaired γC hole polymerization site. Although the amino acid residue that was replaced (Asp 364 in the γ chain) was the same in the fibrinogens, their polymerization properties and thus structures were quite different. When treated with thrombin, the γD364A fibrinogen was capable of forming a fibrin clot, while γD364H was not (*32*). The interactions of γD364A fibrinogen with desA-NDSK resembled closely those of γD364H fibrinogen. The rupture force peaks were detected at 44 ± 7, 72 ± 11, and 105 ± 17 pN (Figure 3g). When 0.1 mM FpB was added to the interacting desA-NDSK and γD364A fibrinogen, the resulting force spectrum was similar to the force spectrum of γD364H and desA-NDSK in the presence of FpB (compare panels e and h of Figure 3). The interaction of γD364A with thrombin-treated desA-NDSK (Figure 3i) was very similar to the interaction shown by γD364H (Figure 3d). Finally, there were almost no interactions between the γD364A fibrinogen and desAB-NDSK (Figure 3j). These data suggest that the interactions between the N-termini of the Bβ chains and fibrinogen are not dependent on the structure and properties of a particular fibrinogen variant.

Although the structure of NDSK is similar to the structure of the fibrinogen E region, they are not identical (*40*). To determine if these structural differences could be responsible for the binding mediated by the N-terminus of the Bβ chain, we replaced desA-NDSK with desA-γD364H fibrin in the binding experiments with γD364H fibrinogen. The binding of γD364H fibrinogen to desA-γD364H fibrin was only slightly different from the binding to desA-NDSK and closely resembled the binding to the NDSK fragment. Three rupture force peaks were detected at 25 ± 2, 61 ± 4, and 96 ± 7 pN, but with a lower interaction probability (Figure 3k). The lower probability could be a result of a difference in protein density between surface-bound desA-fibrin and surface-bound desA-NDSK. These results indicate that the binding interaction mediated by the N-terminus of the Bβ chain does not depend on the unique structural features of the NDSK fragment.

Determining Which Region in Fibrinogen Interacts with the N-Terminus of the Bβ Chain. By using fibrinogen fragments instead of the whole molecule, we eliminated

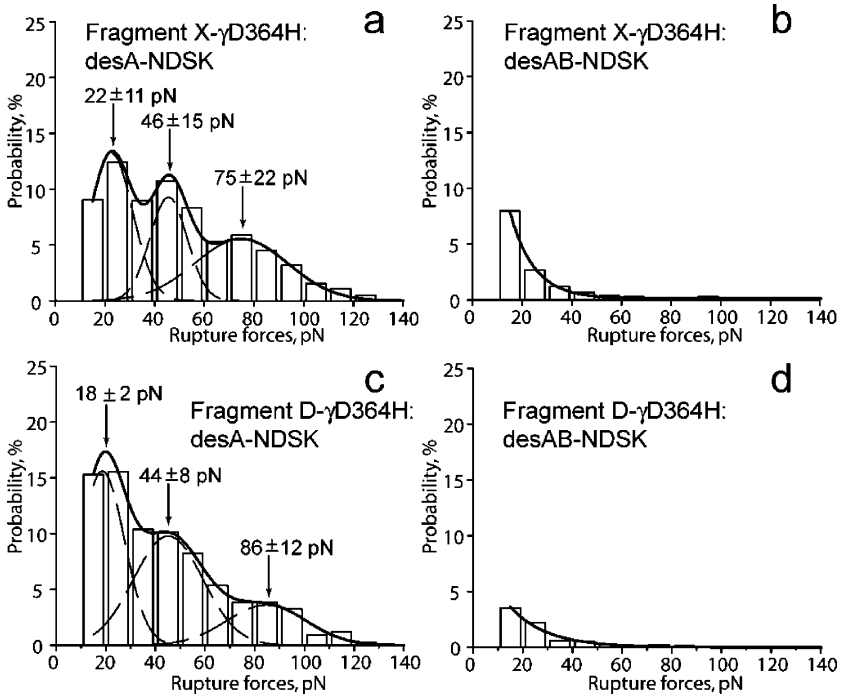

FIGURE 4: Rupture force histograms demonstrating the interactions of fragments X and D from fibrinogen γD364H with desA- and desAB-NDSK fragments. The rupture forces were arranged into histograms with 10 pN wide bins and normalized by the total number of counts (n) for each experimental condition: (a and b) interactions of fragment X from fibrinogen γD364H with desA-NDSK ($n = 3501$) and desAB-NDSK ($n = 2530$), respectively; and (c and d) interactions of fragment D from fibrinogen γD364H with desA-NDSK ($n = 2050$) and desAB-NDSK ($n = 1785$), respectively.

certain parts of fibrinogen from participating in binding interactions with NDSK. We prepared fragments X (X-γD364H) and D (D-γD364H) from limited trypsin digests of γD364H fibrinogen. Compared to intact fibrinogen, the X-γD364H fragment lacks αC-domains and the N-terminus of the Bβ chain (Figure 1b), while the D-γD364H fragment contains part of the coiled-coil connector and the γC and βC modules, representing the D region of fibrinogen (Figure 1c). A broad spectrum of rupture force was detected for the binding of desA-NDSK to X-γD364H. Rupture forces in the range of 20−130 pN were observed with peaks at 22 ± 11, 46 ± 15, and 75 ± 22 pN, and the cumulative probability of forces of >10 pN was equal to 72 ± 12% (Figure 4a). This binding interaction was similar to the binding interaction of desA-NDSK and γD364H fibrinogen with one notable exception; the strong binding forces with a peak at 111 ± 7 pN for γD364H or at 105 ± 17 pN for γD364A were missing (compare panels b and g of Figure 3 with panel a of Figure 4). Removal of FpB resulted in the almost-complete disappearance of interactions between desAB-NDSK and X-γD364H (Figure 4b), similar to the outcome of other binding experiments in which desAB-NDSK was used (Figure 3c,j). We assigned the binding force of 111 ± 7 pN to interaction of the N-terminus of the Bβ chain with the αC-domain, because these forces were evident in binding of fibrinogen but not fragment X to desA-NDSK, and the main difference between fibrinogen and X fragments was the absence of the αC-domains.

When the X-γD364H fragment was replaced with the D-γD364H fragment, rupture forces in the range of 20−130 pN with three well-defined peaks at 18 ± 2, 44 ± 8, and 86 ± 12 pN were detected (Figure 4c). The cumulative probability of the forces of >10 pN was 78 ± 14%. As with fibrinogen and X fragments, the removal of FpB from desA-NDSK completely abrogated binding of the desAB-NDSK and D-γD364H fragments (Figure 4d). Since removal of the center of the fibrinogen molecule and one distal part (which occurs during transformation of X-γD364H into D-γD364H) did not change the force spectrum (compare panels a and c of Figure 4), we conclude that the distal part of the fibrinogen molecule corresponding to the D region was responsible for the interaction with the N-terminus of the Bβ chain of the desA-NDSK fragment.

Analysis of NDSK−NDSK Binding. We assessed the binding of NDSK fragments to each other because we wanted to know if the N-terminus of the Bβ chain was capable of interacting with central region E of another molecule. We examined interactions between NDSK fragments that differed in their fibrinopeptide content. Interaction of desA-NDSK with NDSK or desA-NDSK produced a force spectrum with binding interactions in the range of 20−120 pN (Figure 5a,b). When both fibrinopeptides were removed from both interacting NDSK fragments (Figure 5c) or from only one NDSK fragment (Figure 5d), the interaction was weak, almost nonexistent. The binding of desA-NDSK to desAB-NDSK and NDSK to NDSK was different from the binding of other pairs of NDSK fragments. This binding was characterized by a broad asymmetrical peak at ∼25 pN, with a shoulder that extended well up to 140 pN (Figure 5e,f). The data suggest that NDSK fragments are capable of interacting with each other, and this interaction clearly depends on whether fibrinopeptides are present or absent in the NDSK fragments.

Effect of GPRP and GHRP Peptides on the Interaction of DesA-NDSK with γD364H Fibrinogen. Because 'B' knob exposure led to abrogation of interactions between γD364H fibrinogen and desA-NDSK, we ruled out the involvement of B:b or A:b knob−hole interactions in this binding. Nevertheless, to substantiate this finding, we studied the

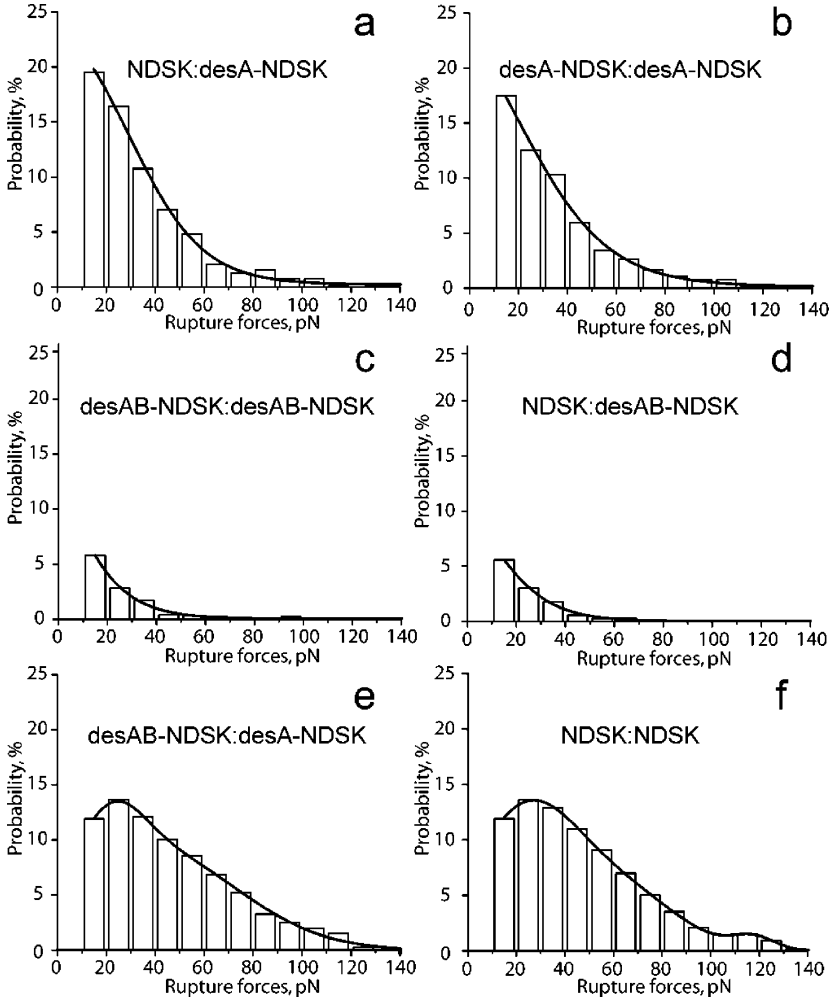

FIGURE 5: Rupture force histograms demonstrating the interactions between different NDSK fragments. The rupture forces were arranged into histograms with 10 pN wide bins and normalized by the total number of counts (n) for each experimental condition: (a and b) interactions of desA-NDSK with NDSK ($n = 2379$) and desA-NDSK ($n = 2224$), respectively; (c−e) interactions of desAB-NDSK with desAB-NDSK ($n = 1275$), NDSK ($n = 1633$), and desA-NDSK ($n = 1167$), respectively; and (f) interactions between the surfaces both coated with NDSK ($n = 1705$).

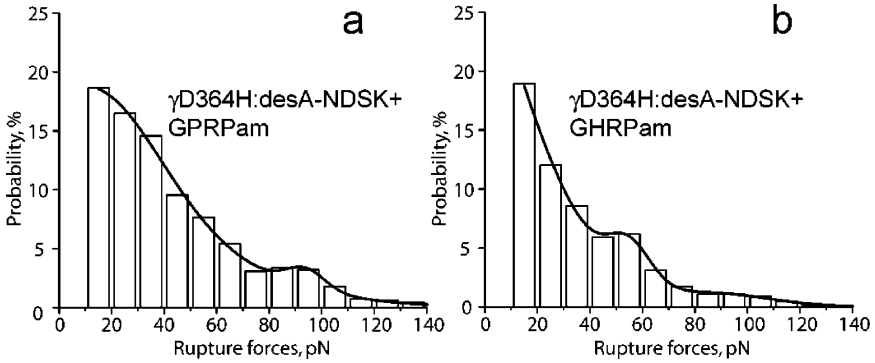

FIGURE 6: Rupture force histograms demonstrating the effects of GPRP ($n = 1620$) (a) and GHRP ($n = 1214$) (b) peptides on the interactions between fibrinogen variant γD364H and desA-NDSK. The rupture forces were arranged into histograms with 10 pN wide bins and normalized by the total number of counts (n) for each experimental condition.

effect of GPRP or GHRP peptides on the binding of the desA-NDSK fragment to γD364H fibrinogen. With γD364H fibrinogen, both peptides were most likely binding to the polymerization hole located in the βC module, because the polymerization hole in the γC module was incapable of peptide binding. It was shown previously that GPRP and GHRP are capable of binding to the βC hole (*41*, *42*). The peptides were introduced into the reaction chamber at a final concentration of 5 mM, and the binding of desA-NDSK with γD364H fibrinogen was examined (Figure 6a,b). The introduction of either peptide changed the binding but did not stop it, like the removal of FpB did. In the presence of peptides, the interactions became less defined, but the cumulative probability of binding forces was changed insignificantly (60−85%), resulting in a moderate inhibitory effect somewhat similar to what was seen with added FpA (Figure 3f). The change in force spectra when peptides bind to the D region was another indication that the D region was

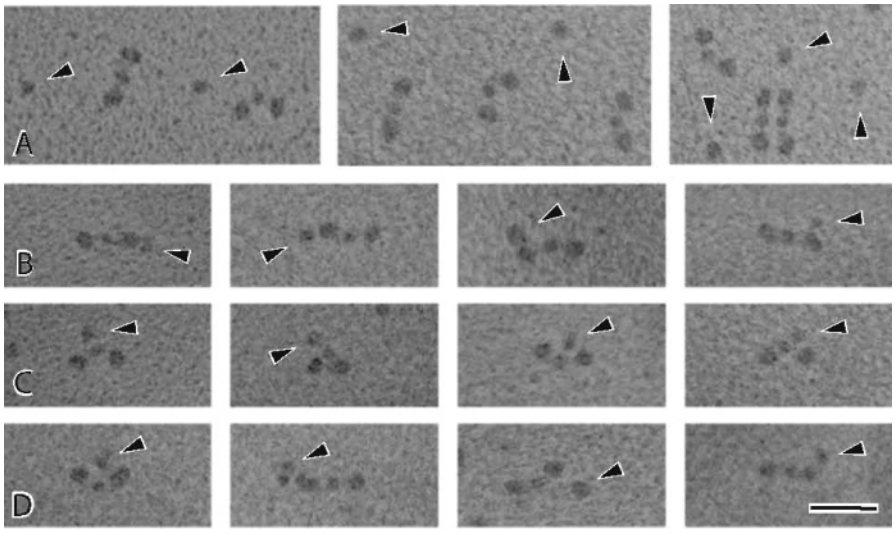

FIGURE 7: Transmission electron micrographs of rotary shadowed complexes of γD364H fibrinogen with NDSK. The γD364H fibrinogen is no different in appearance than control fibrinogen, while the NDSK appears as a single nodule. The NDSK fragments are denoted with arrowheads. (A) γD364H fibrinogen with desAB-NDSK. No complexes are present, so the appearance of the separated γD364H fibrinogen and NDSK can be observed. (B−D) γD364H fibrinogen with desA-NDSK. In panel B, the desA-NDSK is near the end of the γD364H fibrinogen. In panel C, the desA-NDSK is near the middle of the γD364H fibrinogen. In panel D, the desA-NDSK is farther from the backbone of the γD364H fibrinogen, indicating complexes of the N-terminus of the Bβ chain of desA-NDSK and the αC-domains of the γD364H fibrinogen. In some cases, a smaller nodule (αC-domain) is present adjacent to the larger nodule (NDSK). The magnification bar is 50 nm.

involved in the interaction between desA-NDSK and γD364H fibrinogen.

Electron Microscopy Analysis of the NDSK Fragment and γD364H Fibrinogen. To confirm the ability of the NDSK fragments to bind γD364H fibrinogen in solution and to localize the interacting molecular regions, we visualized NDSK−fibrinogen complexes by transmission electron microscopy. Rotary shadowing in the presence of added glycerol was used to minimize protein−surface interactions (*37*). γD364H fibrinogen was mixed with desA-NDSK at a 1:1 molar ratio. γD364H fibrinogen appeared to be similar to control fibrinogen (Figure 7A). desA-NDSK appeared as a single nodule (Figure 7A, arrowheads). Three types of complexes were observed. There were (a) complexes with the desA-NDSK near the ends of γD364H fibrinogen (Figure 7B) or (b) complexes with the desA-NDSK near the middle region of the γD364H fibrinogen (Figure 7C). In both cases, most complexes displayed a small gap between the NDSK nodule and the fibrinogen, suggesting that the extended N-terminus of the Bβ chain acts as a spacer between the two. (c) Other complexes with a longer spacing between desA-NDSK and γD364H fibrinogen were also observed (Figure 7D), likely corresponding to interactions between the N-terminus of the Bβ chain of desA-NDSK and the αC-domains of γD364H fibrinogen. Even with very low ratios of desA-NDSK, complexes of these three types were observed. In contrast, few complexes were observed with desAB-NDSK and γD364H fibrinogen (Figure 7A).

DISCUSSION

Previously, using laser tweezers, we determined the binding forces between single molecules of fibrin NDSK fragments and fibrinogen, which were shown to reflect exclusively the 'A' knob and 'a' hole interactions (*29*). We hypothesized that strong 'A' knob and 'a' hole interactions were masking other weaker interactions in our experimental system. By making knob−hole interactions unavailable, we expected to eliminate their masking effect. That was achieved by using recombinant fibrinogen γD364H and its fragments containing a nonfunctional 'a' hole (*32*). Indeed, by eliminating the binding of 'A' knob to 'a' hole, we discovered previously unknown, specific interactions between NDSK or desA-NDSK fragments and γD364H. These interactions were dependent on the availability of uncleaved fibrinopeptides, particularly FpB. Although the cleavage of FpA also affected these interactions, only removal of FpB completely eliminated them, leading us to the conclusion that we discovered interactions independent of the known knob−hole mechanism. This was further confirmed by the lack of an inhibition effect of peptides mimicking the polymerization knobs (GPRP and GHRP). We have shown that these interactions were not peculiar to the structure of NDSK fragments or γD364H fibrinogen because binding remained when desA-NDSK was replaced with desA-fibrin and γD364H fibrinogen was replaced with γD364A fibrinogen.

Taken alone, a rupture force spectrum cannot be used to prove the specificity of interactions because specific and nonspecific interactions may overlap (*28*, *38*, *43*). We demonstrated the specificity of the interactions by inhibiting them with free FpB or by cleaving FpB.

Studies of the binding modulated by the N-terminus of the Bβ chain revealed the complex nature of this interaction. The finding of 111 ± 7 pN rupture forces arising from the disruption of the bond between FpB and the αC-domain, also confirmed by electron microscopy, is in good agreement with the known dependence of the dissociation of the αC-domains from the central E region of the fibrin monomer upon fibrinopeptide release (*36*, *44*). However, no part of the fibrinogen molecule was identified before as a binding site for the αC-domains. We propose that the αC-domains are bound to the center of the fibrinogen molecule by interacting with FpB or with FpB together with other parts

of the fibrin β chain. When FpB is cleaved, the binding site is destroyed and the αC-domains are released from the center of the fibrin monomer, thus enabling participation of the αC-domain in the lateral aggregation of protofibrils and interactions with other proteins and cells (*44*, *45*).

In addition to binding to the αC-domains, we found that the N-terminus of the Bβ chain binds to the D region of the fibrinogen molecule. This binding was slightly affected by the addition of GPRP or GHRP peptides, which could be a result of conformational changes in the D region (*41*, *42*). Therefore, it is conceivable that the N-terminus of the Bβ chain is interacting with the βC module in the D region.

Because the N-terminus of the Bβ chain is an integral part of the central E region of the fibrinogen molecule, we investigated the binding of NDSK fragments to each other. The interactions between NDSK fragments were dependent on the presence of intact fibrinopeptides, indicating that the removal of fibrinopeptides alters the exposure of reactive sites. Since the conformation of the N-terminus of the Bβ chain and its location in fibrinogen remain unknown (*5*, *27*), we can conclude only that the N-terminus of the Bβ chain is capable of weak binding to the central E region of the same or another fibrin(ogen) molecule.

While the physiological implication of binding of the αC-domain to uncleaved FpB is clear (*44*), the importance of binding of the N-terminus of the Bβ chain to the D region is less obvious. There is evidence that the N-terminus of the Bβ chain affects fibrin polymerization before FpB cleavage. For example, batroxobin-catalyzed polymerization (no FpB cleaved, only the 'A' knob exposed) of fibrinogen with alterations in the N-terminus of the Bβ chain is impaired (*30*, *46*, *47*). Interaction of the N-terminus of the Bβ chain with the D region of the same or another fibrinogen molecule could serve as a mechanism by which FpB cleavage by thrombin is delayed until formation of the desA-fibrin polymer. The weak intramolecular interactions of the N-terminus of the Bβ chain could be important also for proper folding and maintenance of the native conformation of fibrinogen needed for its functions as well as for intracellular processes such as fibrinogen post-translational modification, sorting, trafficking, and secretion (*48*, *49*).

In conclusion, we discovered and quantified interactions between the N-terminus of the Bβ chain of one molecule and the D region, E region, and αC-domains of the same or another fibrinogen or fibrin molecule. These interactions are dependent on fibrinopeptide availability and involved in the mechanism of dissociation of αC-domains upon fibrinopeptide cleavage and participation of the N-terminus of the Bβ chain in desA-fibrin polymerization.

ACKNOWLEDGMENT

We thank Dr. David Klapper for the synthesis of GPRPAA resin, Dr. Susan Lord for helpful discussions, and Dr. Henry Shuman for access to the laser tweezers instrument and expert assistance with measurements.

REFERENCES

1. Weisel, J. W. (2005) Fibrinogen and fibrin, *Adv. Protein Chem. 70*, 247−299.
2. Roberts, H. R., Stinchcombe, T. E., and Gabriel, D. A. (2001) The dysfibrinogenaemias, *Br. J. Haematol. 114*, 249−257.
3. Browder, T., Folkman, J., and Pirie-Shepherd, S. (2000) The hemostatic system as a regulator of angiogenesis, *J. Biol. Chem. 275*, 1521−1524.
4. Henschen, A., Lottspeich, F., Kehl, M., and Southan, C. (1983) Covalent structure of fibrinogen, *Ann. N.Y. Acad. Sci. 408*, 28−43.
5. Yang, Z., Kollman, J. M., Pandi, L., and Doolittle, R. F. (2001) Crystal structure of native chicken fibrinogen at 2.7 Å resolution, *Biochemistry 40*, 12515−12523.
6. Laudano, A. P., Cottrell, B. A., and Doolittle, R. F. (1983) Synthetic peptides modeled on fibrin polymerization sites, *Ann. N.Y. Acad. Sci. 408*, 315−329.
7. Spraggon, G., Everse, S. J., and Doolittle, R. F. (1997) Crystal Structures of Fragment D From Human Fibrinogen and Its Crosslinked Counterpart From Fibrin, *Nature 389*, 455−462.
8. Kostelansky, M. S., Betts, L., Gorkun, O. V., and Lord, S. T. (2002) 2.8 Å crystal structures of recombinant fibrinogen fragment D with and without two peptide ligands: GHRP binding to the "b" site disrupts its nearby calcium-binding site, *Biochemistry 41*, 12124−12132.
9. Yang, Z., Mochalkin, I., and Doolittle, R. F. (2000) A model of fibrin formation based on crystal structures of fibrinogen and fibrin fragments complexed with synthetic peptides, *Proc. Natl. Acad. Sci. U.S.A. 97*, 14156−14161.
10. Olexa, S. A., and Budzynski, A. Z. (1981) Localization of a fibrin polymerization site, *J. Biol. Chem. 256*, 3544−3549.
11. Ferry, J. D. (1952) The mechanism of polymerization of fibrinogen, *Proc. Natl. Acad. Sci. U.S.A. 38*, 566−569.
12. Hantgan, R. R., and Hermans, J. (1979) Assembly of fibrin. A light scattering study, *J. Biol. Chem. 254*, 11272−11281.
13. Erickson, H. P., and Fowler, W. E. (1983) Electron microscopy of fibrinogen, its plasmic fragments and small polymers, *Ann. N.Y. Acad. Sci. 408*, 146−163.
14. Weisel, J. W., and Nagaswami, C. (1992) Computer modeling of fibrin polymerization kinetics correlated with electron microscope and turbidity observations: Clot structure and assembly are kinetically controlled, *Biophys. J. 63*, 111−128.
15. Weisel, J. W., Veklich, Y., and Gorkun, O. (1993) The sequence of cleavage of fibrinopeptides from fibrinogen is important for protofibril formation and enhancement of lateral aggregation in fibrin clots, *J. Mol. Biol. 232*, 285−297.
16. Weisel, J. W., Nagaswami, C., and Makowski, L. (1987) Twisting of fibrin fibers limits their radial growth, *Proc. Natl. Acad. Sci. U.S.A. 84*, 8991−8995.
17. Baradet, T. C., Haselgrove, J. C., and Weisel, J. W. (1995) Three-dimensional reconstruction of fibrin clot networks from stereoscopic intermediate voltage electron microscope images and analysis of branching, *Biophys. J. 68*, 1551−1560.
18. Higgins, D. L., Lewis, S. D., and Shafer, J. A. (1983) Steady state kinetic parameters for the thrombin-catalyzed conversion of human fibrinogen to fibrin, *J. Biol. Chem. 258*, 9276−9282.
19. Blomback, B., Hessel, B., Hogg, D., and Therkildsen, L. (1978) A two-step fibrinogen−fibrin transition in blood coagulation, *Nature 275*, 501−505.
20. Shen, L. L., Hermans, J., McDonagh, J., and McDonagh, R. P. (1977) Role of fibrinopeptide B release: Comparison of fibrins produced by thrombin and Ancrod, *Am. J. Physiol. 232*, H629−H633.
21. Weisel, J. W. (1986) Fibrin assembly. Lateral aggregation and the role of the two pairs of fibrinopeptides, *Biophys. J. 50*, 1079−1093.
22. Dyr, J. E., Blomback, B., Hessel, B., and Kornalik, F. (1989) Conversion of fibrinogen to fibrin induced by preferential release of fibrinopeptide B, *Biochim. Biophys. Acta 990*, 18−24.
23. Shainoff, J. R., and Dardik, B. N. (1979) Fibrinopeptide B and aggregation of fibrinogen, *Science 204*, 200−202.
24. Moskowitz, K. A., and Budzynski, A. Z. (1994) The (DD)E complex is maintained by a composite fibrin polymerization site, *Biochemistry 33*, 12937−12944.
25. Pandya, B. V., Gabriel, J. L., O'Brien, J., and Budzynski, A. Z. (1991) Polymerization site in the β chain of fibrin: Mapping of the Bβ 1−55 sequence, *Biochemistry 30*, 162−168.
26. Siebenlist, K. R., DiOrio, J. P., Budzynski, A. Z., and Mosesson, M. W. (1990) The polymerization and thrombin-binding properties of des-(Bβ1−42)-fibrin, *J. Biol. Chem. 265*, 18650−18655.
27. Pechik, I., Yakovlev, S., Mosesson, M. W., Gilliland, G. L., and Medved, L. (2006) Structural Basis for Sequential Cleavage of Fibrinopeptides upon Fibrin Assembly, *Biochemistry 45*, 3588−3597.

28. Litvinov, R. I., Bennett, J. S., Weisel, J. W., and Shuman, H. (2005) Multi-step fibrinogen binding to the integrin αIIbβ$_3$ detected using force spectroscopy, *Biophys. J. 89*, 2824−2834.
29. Litvinov, R. I., Gorkun, O. V., Owen, S. F., Shuman, H., and Weisel, J. W. (2005) Polymerization of fibrin: Specificity, strength, and stability of knob-hole interactions studied at the single-molecule level, *Blood 106*, 2944−2951.
30. Lord, S. T., and Gorkun, O. V. (2001) Insight from studies with recombinant fibrinogens, *Ann. N.Y. Acad. Sci. 936*, 101−116.
31. Gorkun, O. V., Veklich, Y. I., Weisel, J. W., and Lord, S. T. (1997) The conversion of fibrinogen to fibrin: Recombinant fibrinogen typifies plasma fibrinogen, *Blood 89*, 4407−4414.
32. Okumura, N., Gorkun, O. V., and Lord, S. T. (1997) Severely impaired polymerization of recombinant fibrinogen γ-364 Asp−His, the substitution discovered in a heterozygous individual, *J. Biol. Chem. 272*, 29596−29601.
33. Blomback, B., Hessel, B., Iwanaga, S., Reuterby, J., and Blomback, M. (1972) Primary structure of human fibrinogen and fibrin. I. Clevage of fibrinogen with cyanogen bromide. Isolation and characterization of NH_2-terminal fragments of the ("A") chain, *J. Biol. Chem. 247*, 1496−1512.
34. Blomback, B., Hessel, B., and Hogg, D. (1976) Disulfide bridges in NH_2-terminal part of human fibrinogen, *Thromb. Res. 8*, 639−658.
35. Hessel, B., Makino, M., Iwanaga, S., and Blomback, B. (1979) Primary structure of human fibrinogen and fibrin. Structural studies on NH_2-terminal part of Bβ chain, *Eur. J. Biochem. 98*, 521−534.
36. Veklich, Y. I., Gorkun, O. V., Medved, L. V., Nieuwenhuizen, W., and Weisel, J. W. (1993) Carboxyl-terminal portions of the α chains of fibrinogen and fibrin. Localization by electron microscopy and the effects of isolated α C fragments on polymerization, *J. Biol. Chem. 268*, 13577−13585.
37. Tyler, J. M., and Branton, D. (1980) Rotary shadowing of extended molecules dried from glycerol, *J. Ultrastruct. Res. 71*, 95−102.
38. Leckband, D. E., Schmitt, F. J., Israelachvili, J. N., and Knoll, W. (1994) Direct force measurements of specific and nonspecific protein interactions, *Biochemistry 33*, 4611−4624.
39. Evans-Nguyen, K. M., Tolles, L. R., Gorkun, O. V., Lord, S. T., and Schoenfisch, M. H. (2005) Interactions of thrombin with fibrinogen adsorbed on methyl-, hydroxyl-, amine-, and carboxyl-terminated self-assembled monolayers, *Biochemistry 44*, 15561−15568.
40. York, J. L. (1983) Comparative study of the iodination of tyrosines in the amino terminal domain of fibrinogen and in N-DSK and fibrin-N-DSK, *Thromb. Res. 31*, 203−209.
41. Kostelansky, M. S., Bolliger-Stucki, B., Betts, L., Gorkun, O. V., and Lord, S. T. (2004) Bβ Glu397 and Bβ Asp398 but not Bβ Asp432 are required for "B:b" interactions, *Biochemistry 43*, 2465−2474.
42. Betts, L., Merenbloom, B. K., and Lord, S. T. (2006) The structure of fibrinogen fragment D with the 'A' knob peptide GPRVVE, *J. Thromb. Haemostasis 4*, 1139−1141.
43. Leckband, D. (2000) Measuring the forces that control protein interactions, *Annu. Rev. Biophys. Biomol. Struct. 29*, 1−26.
44. Gorkun, O. V., Veklich, Y. I., Medved, L. V., Henschen, A. H., and Weisel, J. W. (1994) Role of the αC-domains of fibrin in clot formation, *Biochemistry 33*, 6986−6997.
45. Belkin, A. M., Tsurupa, G., Zemskov, E., Veklich, Y., Weisel, J. W., and Medved, L. (2005) Transglutaminase-mediated oligomerization of the fibrin(ogen) αC-domains promotes integrin-dependent cell adhesion and signaling, *Blood 105*, 3561−3568.
46. Moen, J. L., Gorkun, O. V., Weisel, J. W., and Lord, S. T. (2003) Recombinant Bβ Arg14His fibrinogen implies participation of N-terminus of Bβ chain in desA fibrin polymerization, *Blood 102*, 2466−2471.
47. Hirota-Kawadobora, M., Kani, S., Terasawa, F., Fujihara, N., Yamauchi, K., Tozuka, M., and Okumura, N. (2005) Functional analysis of recombinant Bβ15C and Bβ15A fibrinogens demonstrates that Bβ15G residue plays important roles in FPB release and in lateral aggregation of protofibrils, *J. Thromb. Haemostasis 3*, 983−990.
48. Brennan, S. O., Fellowes, A. P., and George, P. M. (2001) Molecular mechanisms of hypo- and afibrinogenemia, *Ann. N.Y. Acad. Sci. 936*, 91−100.
49. Neerman-Arbez, M. (2006) Molecular basis of fibrinogen deficiency, *Pathophysiol. Haemostasis Thromb. 35*, 187−198.

BI061430Q